

Dark optical lattice of ring traps for cold atoms

Emmanuel Courtade, Olivier Houde, Jean-François Clément, Philippe Verkerk, and Daniel Hennequin*
*Laboratoire de Physique des Lasers, Atomes et Molécules, UMR CNRS, Centre d'Études et de Recherche Lasers et Applications,
 Université des Sciences et Technologies de Lille, F-59655 Villeneuve d'Ascq cedex, France*

(Received 22 May 2006; published 20 September 2006)

We propose an optical lattice for cold atoms made of a one-dimensional stack of dark ring traps. It is obtained through the interference pattern of a standard Gaussian beam with a counterpropagating hollow beam obtained using a setup with two conical lenses. The traps of the resulting lattice are characterized by a high confinement and a filling rate much larger than unity, even if loaded with cold atoms from a magneto-optical trap. We have implemented this system experimentally, and demonstrated its feasibility. Applications in statistical physics, quantum computing, and Bose-Einstein condensate dynamics are conceivable.

DOI: [10.1103/PhysRevA.74.031403](https://doi.org/10.1103/PhysRevA.74.031403)

PACS number(s): 32.80.Pj, 39.25.+k

Optical lattices provide a versatile tool to study the dynamical properties of cold and ultracold atoms. They are presently the topic of intense research activity, in particular because they represent an outstanding toy model for various domains. In statistical physics, cold atoms in optical lattices, through their tunability, made possible the observation of the transition between Gaussian and power-law tail distributions, in particular the Tsallis distributions [1]. Condensed matter systems and strongly correlated cold atoms in optical lattices offer deep similarities, as in the superfluid–Mott-insulator quantum phase transition [2], in the Tonks-Girardeau regime [3] or for the emergence of a macroscopic current in periodic potentials [4]. In quantum computing, optical lattices appear to be an efficient implementation of a Feynman universal quantum simulator [5], and are among the most promising candidates for the realization of a quantum computer [6].

One of the main advantages of the optical lattices is their high flexibility. By varying the shape of the lattice, a wide range of configurations is reached. Currently, many studies deal with one-dimensional (1D) lattices, in particular because quantum effects are stronger in low-dimensional systems [7]. A particularly interesting situation concerns 1D lattices with periodic boundary conditions, because many new effects appear [8]. Recently, an experimental implementation has been proposed, where the lattice sites are distributed along rings [9]. In a more complex configuration, the sites themselves could have the shape of a ring, allowing, e.g., the study of solitons in 1D Bose-Einstein condensates (BECs) with periodic boundary conditions [10] or atomic-phase interferences between such BECs [11]. Experimental realization of such 1D rings is still an open question, as either a lattice or a single trap. Large magnetic single-ring traps have been produced, in connection with the study of the atomic Sagnac effect [12,13], but their transverse confinement is weak, and they cannot be considered as 1D rings. A more promising proposition is an optical trap built with twisted light obtained from two counterpropagating Laguerre-Gaussian beams with an azimuthal phase dependence [14]. Those authors suggest that an optical lattice of such ring traps could be created by combining several twisted molas-

ses. Such an arrangement has the drawback of trapping the atoms where the light intensity is maximum. This may result in serious perturbations of the atoms due to the trapping beams [15]. In particular, some applications in quantum computation require trapping of the atoms in dark lattices, to make the system robust against decoherence [16]. Contrary to bright lattices, where even a 1D configuration leads to 3D trapping, 1D dark lattices do not trap atoms in 3D: only 3D dark lattices trap atoms in 3D [15]. So far, the only proposal for such a lattice consists in a Gaussian beam making a round trip in a confocal cavity [17]. A difference of waist between the two directions of propagation leads to a lattice of ring traps with $\lambda/2$ periodicity, where λ is the optical wavelength. Such a device has the advantage of generating high light intensity inside the cavity and so deeper traps than with free-propagating beams. But this is obtained at the cost of flexibility: for example, changing the ring radius requires changing the cavity mirrors. These difficulties probably explain why, to our knowledge, this proposal has not yet been realized experimentally.

We propose here a different geometry for a dark lattice of ring traps, obtained from a hollow beam and a counterpropagating Gaussian beam, without any cavity. The radius and the thickness of the rings can be adjusted independently, and due to the stiff edges of the hollow beam, the trap steepness is much larger than in [17]. Finally, the filling rate of each site is much larger than unity, even when loaded with a magneto-optical trap (MOT), unlike 3D dark lattices, which require the use of a BEC. The filling rate should even reach values in excess of 1000 atoms per site if an adequate sequence is used to turn on the lattice.

The paper is organized as follows: We first discuss the principle of the lattice of ring traps, then describe the experimental realization, and finally show preliminary results concerning cold atoms loaded in the lattice.

Each individual trap is a 3D dark ring, and the lattice is a 1D stack of such rings. Thus, the global shape of the potential is a bright full cylinder with a pile of ring wells inside. To obtain this potential, a standard Gaussian beam interferes with a counterpropagating hollow beam with no azimuthal phase dependence [18], unlike the Laguerre-Gaussian beams used, e.g., as waveguides [19]. Both beams have the same blue-detuned frequency, so that the trapping sites correspond to the zero-intensity places. Both beams propagate along the

*Electronic address: daniel.hennequin@univ-lille1.fr

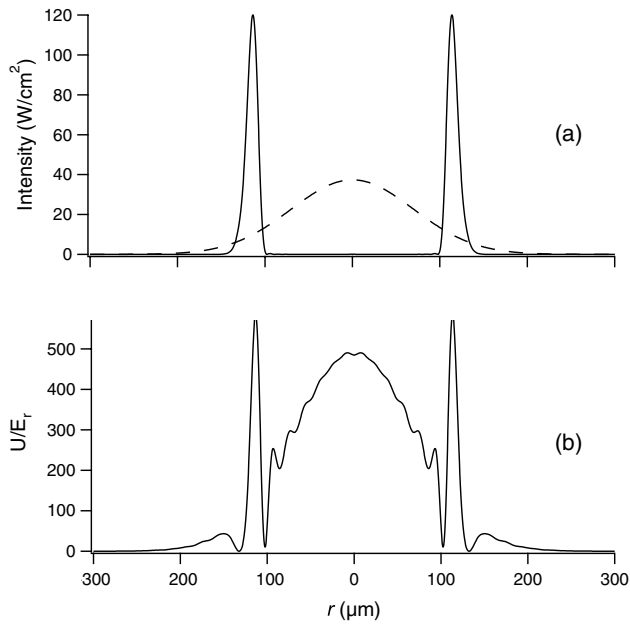


FIG. 1. (a) Theoretical transverse profile of the Gaussian (dashed) and hollow (full) beams used in the experiment. (b) The resulting transverse potential at the bottom of the well. Parameters are those used in the experiments.

z vertical axis, and the hollow beam is a cylindrical beam, with an intensity distribution along the radial direction r as illustrated in Fig. 1(a) (solid line). When the two beams are out of phase, two pairs of zeros of intensity appear symmetrically on each side of the center, at $r=100$ and $130 \mu\text{m}$ on Fig. 1(b), where the two beam intensities are equal. Because of the cylindrical symmetry, these zeros correspond to two concentric rings along the azimuthal direction. In contrast, when the two beams have the same phase, the intensity profile reaches its maximum. This interference pattern results in a potential U which is, in the limit of weak saturation and large detuning, proportional to the light intensity I :

$$U = \frac{\hbar \Gamma^2 I}{8 \Delta I_S}, \quad (1)$$

where Δ is the detuning, I_S the saturation intensity, and Γ the width of the atomic transition. Because the outer ring is shallow, only the inner ring, at $r=100 \mu\text{m}$, is a trap.

A hollow beam as described above is easily produced by a conical lens [18]. Conical lenses are extensively used to produce Bessel-Gauss [20] or annular beams [21,22]. To generate an annular hollow beam, we use a converging lens L to shape the incident Gaussian beam, and then a conical lens. Each incident ray is deviated toward the optical axis z by the conical lens, and thus the incident Gaussian beam is transformed into a ring [18]. A second conical lens is used to collimate the radius r of the ring, so that after this second lens, r becomes constant with z . The resulting hollow beam has a radius r which depends only on the distance between the two conical lenses, while its thickness Δr depends on the focal length of L . Thus r and Δr are adjustable independently.

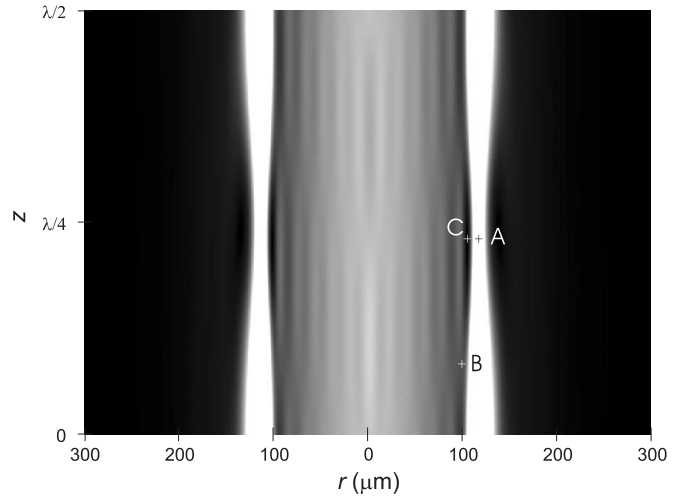


FIG. 2. 2D representation of the potential as a function of the radius r and the longitudinal coordinate z . The complete potential has a revolution symmetry around the axis $r=0$. Parameters are those of Fig. 1. Note that the scales along z and r are different. Dark corresponds to a zero potential. Significance of points A, B, and C is given in the text.

The potential is obtained by focusing the Gaussian beam and the counterpropagating hollow beam at the same point, so that the wave surfaces are planes perpendicular to the propagation axis. The resulting potential has a periodicity of $\lambda/2$, with a shape depending locally on the phase ϕ between the two beams. It is illustrated through the theoretical plots of Figs. 1(b) and 2 where, for the sake of simplicity, we used the parameters of the experimental demonstration described below: the hollow and Gaussian intensities are, respectively, $I_H=14 \text{ mW}$ and $I_G=11.5 \text{ mW}$ [Fig. 1(a)], with $\Delta/2\pi=70 \text{ GHz}$. Figure 1(b) shows the potential transverse profile at the bottom of the wells. The geometry of the ring appears clearly, with a confinement of the order of $r/10$ for $U < 200E_r$, and a height for the external barrier of $580E_r$, where E_r is the recoil energy. Secondary minima, originating in the residual diffraction produced by the mask used to remove inner rings of the hollow beam [18], appear inside the main ring, but because of their weak depth, they should not be annoying in most applications.

A better understanding of the potential distribution can be obtained from Fig. 2, where U is plotted in gray scale versus r and z . The potential is periodic along z , with a period $\lambda/2$. Atoms with low enough energy are confined in a torus with a half-ellipse cross section with axes of the order of 0.1 and $10 \mu\text{m}$, corresponding on the figure to the dark zone at the point C. The height of the external barrier varies with z . The minimum height $U_A=580E_r$, at point A of Fig. 2, occurs at the same z as the bottom of the main well [Fig. 1(b)]. The internal barrier has a channel structure, with the lowest pass at point B (Fig. 2), at a height of $U_B=200E_r$, between two successive longitudinal sites.

The number of atoms that we should be able to put in each site of this lattice depends of course on the density of the cloud of cold atoms used to load the lattice, but also on the spatial overlap between the cloud and the lattice. In particular, when the atoms are loaded from a MOT, the capture

volume of the lattice is decisive for its filling rate. In the present case, the capture volume is determined by the hollow beam diameter, which may be chosen as several hundreds of micrometers. For example, with $r=100\ \mu\text{m}$ (Fig. 2) and an initial cloud of radius 1 mm, 1.5% of the initial atoms are inside the hollow beam. Thus, if the lattice is loaded with a cloud of 10^8 atoms in $4\ \text{mm}^3$, which are the typical characteristics obtained from a MOT, 1.5×10^6 atoms are loaded in 2000 sites, leading to a filling rate much larger than 1.

To test the feasibility of this lattice, we have implemented an experiment with the characteristics described above. Cesium atoms are initially cooled in a standard MOT with a -3Γ detuning from resonance. At time $t=-40\ \text{ms}$, the magnetic field is turned off, while at time $t=-30\ \text{ms}$, the detuning is increased to -5Γ and the trap beam intensity is decreased: this sequence allows us to obtain at time $t=0$ a $40\ \mu\text{K}$ molasses, corresponding to an energy of $200E_r$, with 10^8 atoms in typically $4\ \text{mm}^3$.

The hollow and Gaussian beams are produced by two laser diodes injected by a single master laser diode in an extended cavity, which ensures the same frequency for both beams. For this demonstration, the beams are tuned 70 GHz above the atomic transition. In these conditions, the power of the Gaussian and hollow beams, respectively, 11.5 and 14 mW, is sufficient to reach the needed potential depth of $200E_r$. The Gaussian beam has a minimum waist of $140\ \mu\text{m}$, located at the level of the MOT. The axicon setup is mounted on an optical rail, to guarantee good stability of the beam. The incident beam is collimated with a waist equal to $645\ \mu\text{m}$. The two conical lenses, with a vertex angle of 2° , are separated by a distance of about 10 cm, adjusted to obtain $r=1\ \text{mm}$. The L focal length of 500 mm leads to $\Delta r=100\ \mu\text{m}$. A telescope located just before the trap reduces these values to $r \approx 100\ \mu\text{m}$ and $\Delta r \approx 10\ \mu\text{m}$. We obtain in the MOT a transverse distribution of the hollow beam which is in excellent agreement with the theoretical one.

To load the cold atoms inside the lattice, the latter is turned on at a time $t < 0$, so that, when the molasses is switched off, the atoms are already distributed inside the wells. At time $t=0$, the atoms start to fall under the effect of gravity, except for those that are trapped in the lattice. The free atoms need typically 25 ms to quit the camera field of view, so that for $t > 25\ \text{ms}$, only atoms interacting with the optical lattice remain. To observe the atoms, we switch on during 1 ms the trap laser beams near resonance, and we used a low-noise cooled charge-couple device camera to detect the fluorescence emitted by the atoms. A typical picture is shown in Fig. 3. As the resolution of the imaging setup is about $10\ \mu\text{m}$, individual rings separated by $\lambda/2$ cannot be distinguished. On the contrary, the picture resolves the transverse distribution characterized by two maxima resulting from the side view of the rings. The dashed line is the theoretical distribution obtained when the potential is approximated by a double Gaussian curve. Thus the experimental distribution is less contrasted because the inner walls of the actual wells are flatter than the outer ones.

Figure 4 shows the evolution of the population of the lattice as a function of the time, for the above parameters. The points are obtained by integrating the experimental pictures along the z axis. In order to test the robustness of the

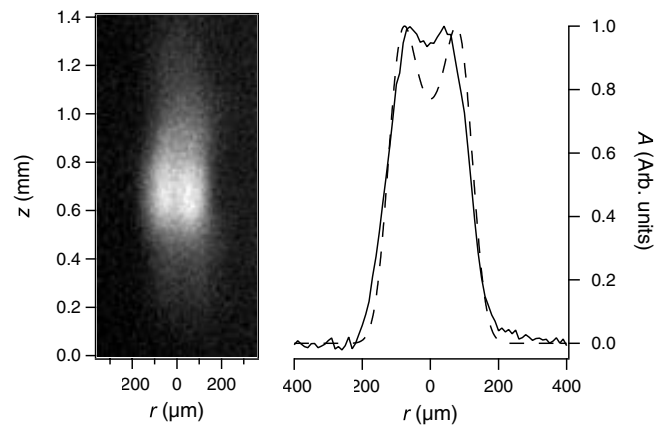


FIG. 3. Left, side view of the lattice obtained by taking a snapshot of the fluorescence of the atoms in the lattice at time $t=40\ \text{ms}$. Right, the corresponding transverse distribution (solid line) and a rough estimate of the theoretical distribution (dashed line). The two-bump structure reveals the annular structure of the traps.

procedure, eight measurements have been done for each point on the abscissa. Figure 4 shows that the number of atoms decreases exponentially with time. The fit to an exponential (solid line in Fig. 4) gives a lifetime of 30 ms. This value is in good agreement with the theoretical lifetime of the atoms resulting from collisions and spontaneous emission. The number of atoms in the lattice is also in good agreement with the theoretical one: after 40 ms, there are still 30 000 atoms. Assuming that these atoms are localized in about 700 lattice sites, we reach a filling rate of 40 atoms per site. Note that, actually, we have no direct proof of the localization of the atoms, but only the periodic optical potential can prevent the atoms from falling. However, only a direct observation of atom localization, through, e.g., Bragg diffraction, would demonstrate unambiguously that atoms are trapped in the lattice.

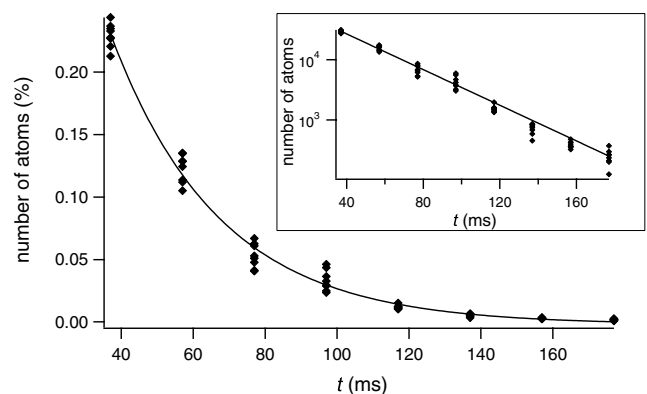


FIG. 4. Number of atoms in the lattice versus time. The main plot is on a linear scale, and the number of atoms is given as a percentage of the molasses population. The solid line corresponds to the fit by an exponential with a decay time $\tau=30\ \text{ms}$. In the inset, the same results are shown on a logarithmic scale, with the absolute number of atoms. In both cases, points are experimental.

In conclusion, we propose here a lattice geometry consisting of a 1D stack of ring traps, and show its experimental feasibility. The experimental setup remains relatively simple, because the lattice is created from only one pair of beams and it does not need any cavity, contrary to the propositions in, respectively, [14,17]. The other characteristics of this lattice are high confinement of the atoms due to the stiff walls of the trapping sites; large capture volume and filling rate, due to the independence of the torus radius and thickness; and weak interaction between light and atoms, as the traps are dark. We implemented such a lattice experimentally, and loaded it directly from a MOT. We measure the lifetime of the atoms in the lattice of 30 ms. Although we have no direct evidence of the localization of the atoms in the lattice sites, this demonstrates the feasibility of this system. The lifetime should be improved by changing some parameters which were not optimized for this feasibility demonstration. For example, a decrease of the initial temperature of the atoms in the molasses by an adequate cooling sequence leads to relatively deeper traps. An increase of the detuning Δ of the lattice, which requires more intense laser sources, reduces the spontaneous emission. Finally, a decrease of the pressure of the thermal atoms, through, e.g., the use of a double cell, improves the collision rate. Each of these enhancements will contribute to lengthening the lifetime of the atoms in the lattice. If better filling rates are necessary, it would also be possible to increase it. Indeed, when the lattice is switched

on, many atoms are heated on the lattice axis, because this axis corresponds to a maximum of the potential. To avoid these extra losses, we plan to switch on the lattice in two steps. First, the hollow beam is switched on just after the trap beams are switched off, so that the atoms inside the beam are trapped and remain in the cylinder. Then, the Gaussian beam is switched on progressively, so that the atoms are adiabatically pushed into the ring traps. This precaution prevents the atoms from being heated by a sudden increase of the potential.

Finally, it would be interesting to study the dynamics of the atoms in this lattice geometry. Moreover, this lattice could be used in systems where interactions between atoms in the same or neighboring sites are required, or when periodic limit conditions are necessary.

The Laboratoire de Physique des Lasers, Atomes et Molécules is Unité Mixte de Recherche de l'Université de Lille 1 et du CNRS (UMR 8523). The Centre d'Études et de Recherches Lasers et Applications (CERLA) is supported by the Ministère chargé de la Recherche, the Région Nord-Pas de Calais and the Fonds Européen de Développement Économique des Régions. The group is supported by the Institut de Recherche sur les Composants logiciels et matériels pour l'Information et la Communication Avancée (IRCICA).

-
- [1] P. Douglas, S. Bergamini, and F. Renzoni, *Phys. Rev. Lett.* **96**, 110601 (2006).
- [2] M. Greiner, O. Mandel, T. Esslinger, T. W. Hänsch, and I. Bloch, *Nature (London)* **415**, 39 (2002).
- [3] B. Paredes, A. Widera, V. Murg, O. Mandel, S. Fölling, I. Cirac, G. V. Shlyapnikov, T. W. Hänsch, and I. Bloch, *Nature (London)* **429**, 277 (2004).
- [4] A. V. Ponomarev, J. Madroñero, A. R. Kolovsky, and A. Buchleitner, *Phys. Rev. Lett.* **96**, 050404 (2006).
- [5] D. Jaksch and P. Zoller, *Ann. Phys.* **315**, 52 (2005).
- [6] O. Mandel, M. Greiner, A. Widera, T. Rom, T. W. Hänsch, and I. Bloch, *Nature (London)* **425**, 937 (2003); K. G. H. Vollbrecht, E. Solano, and J. I. Cirac, *Phys. Rev. Lett.* **93**, 220502 (2004).
- [7] M. Kramer, C. Menotti, L. Pitaevskii, and S. Stringari, *Eur. Phys. J. D* **27**, 247 (2003); T. Stöferle, H. Moritz, C. Shori, M. Köhl, and T. Esslinger, *Phys. Rev. Lett.* **92**, 130403 (2004); M. Cristiani, N. Malossi, M. Jona-Lasinio, M. Anderlini, E. Courtade, and E. Arimondo, *Opt. Express* **12**, 4 (2004).
- [8] C. L. Pando L and E. J. Doedel, *Phys. Rev. E* **71**, 056201 (2005); D. W. Hallwood, K. Burnett, and J. Dunningham, e-print quant-ph/0602025.
- [9] L. Amico, A. Osterloh, and F. Cataliotti, *Phys. Rev. Lett.* **95**, 063201 (2005).
- [10] R. Kanamoto, K. Saito, and M. Ueda, *Phys. Rev. A* **73**, 033611 (2006).
- [11] B. P. Anderson, K. Dholakia, and E. M. Wright, *Phys. Rev. A* **67**, 033601 (2003).
- [12] S. Gupta, K. W. Murch, K. L. Moore, T. P. Purdy, and D. Stamper-Kurn, *Phys. Rev. Lett.* **95**, 143201 (2005).
- [13] A. S. Arnold, C. S. Garvie, and E. Riis, *Phys. Rev. A* **73**, 041606(R) (2006).
- [14] A. R. Carter, M. Babiker, M. Al-Amri, and D. L. Andrews, *Phys. Rev. A* **73**, 021401(R) (2006).
- [15] N. Friedman, A. Kaplan, and N. Davidson, *Adv. At., Mol., Opt. Phys.* **48**, 99 (2002).
- [16] A. Kay, J. K. Pachos, and C. S. Adams, *Phys. Rev. A* **73**, 022310 (2006).
- [17] T. Freegarde and K. Dholakia, *Opt. Commun.* **201**, 99 (2002).
- [18] B. Dépret, Ph. Verkerk, and D. Hennequin, *Opt. Commun.* **211**, 31 (2002).
- [19] K. Bongs, S. Burger, S. Dettmer, D. Hellweg, J. Arlt, W. Ertmer, and K. Sengstock, *Phys. Rev. A* **63**, 031602(R) (2001).
- [20] R. M. Herman and T. A. Wiggins, *J. Opt. Soc. Am. A* **8**, 932 (1991); J. Arlt and K. Dholakia, *Opt. Commun.* **177**, 297 (2000).
- [21] P.-A. Bélanger, *Appl. Opt.* **17**, 1080 (1978).
- [22] I. Manek, Yu. B. Ovchinnikov, and R. Grimm, *Opt. Commun.* **147**, 67 (1998); L. Cacciapuoti, M. de Angelis, G. Pierattini, and G. M. Tino, *Eur. Phys. J. D* **14**, 373 (2001).